JOURNAL OF
HYDRO-METEOROLOGY

Research Article

The trend of erosion and accretion of the western coast of the Mekong Delta, the section from Ca Mau Cape to Kien Giang

Duyen Chau My Nguyen[1], Vy Huynh Thuy Duong[1], Long Ta Bui[1]*

[1] Faculty of Environment and Natural Resources, University of Technology, Vietnam National University, Ho Chi Minh City; nguyenduyen91@hcmut.edu.vn; vy.duonghthuyvy@hcmut.edu.vn; longbt62@hcmut.edu.vn

*Correspondence: longbt62@hcmut.edu.vn; Tel.: +84–918017376

Received: 8 January 2024; Accepted: 06 February 2024; Published: 25 March 2024

Abstract: Natural processes and human-caused activities, including coastal erosion, constantly threaten coastal areas. This phenomenon is dangerous because the permanent loss of land leads to the transformation of the coast. In recent years, coastal erosion has become increasingly complicated in the Mekong Delta, especially in the western coastal area of Cape Ca Mau. This study aims to provide updated results of the changing trend of accretion/erosion of the coastline from Cape Ca Mau to Kien Giang in 2021-2023. Specifically, the rate and area of erosion/accretion considered. Remote sensing and GIS tools are used. As a result, in Ngoc Hien district, Ca Mau, the erosion rate is 55.66 m/year, and the erosion area is 47.21 hectares, ranking highest compared to other districts in the same study area. The results also show that the Kien Giang coastal area has a more moderate erosion process than the accretion process. In contrast, on the coast of the Ca Mau Cape area, the erosion and accretion process are complexly interwoven, especially in the Dat Alluvial Plains area Cape - Ngoc Hien (Ca Mau).

Keywords: Coastal erosion; Landsat8 OLI/TIRS; GIS; Mekong Delta; Ca Mau - Kien Giang.

1. Introduction

Coastal erosion is one of the important issues in coastal management. To adapt to it and prevent it where possible and necessary, it is important to recognize the spatial and temporal scale of the phenomenon as well as its causes [1]. The coastal environment constantly changes due to human activities and various physical processes. This increases environmental degradation, including erosion or accretion along many coastal areas. Coastlines are predicted to face unprecedented pressure this century as climate change causes changes in sea levels, storm patterns, waves, and tides. This forecast of increasing pressure is driving a reassessment of current coastal management practices [2–6]. Due to the special importance of the Mekong Delta to world food security, accretion, erosion, and land loss in this area are the subject of many studies [7, 8].

The decrease in sediment is considered an essential factor causing coastal erosion in the Mekong Delta today [9]. However, human activities cannot be ruled out; for example, sand mining at the river bottom can lead to currents, changing sediment deposition [10]. Mud and sand are trapped behind dams, leading to a decrease in coastal sediment supply, which is considered the overarching cause of decreased sediment supply to the coast, leading to coastal erosion [11–13]. To evaluate hydrodynamics and sediment transport, 2- and 3-dimensional models have been used [14–17]. These studies have focused on clarifying sediment's seasonal distribution and mud dependence on meteorological,

hydrological, oceanographic, tide, wave, and storm surges. To evaluate the scope and extent of sedimentation and erosion processes as well as determine the concentration of suspended matter (SPM) over time, remote sensing methods have been used [18]–[21]. The modelling and remote sensing approaches have highlighted how the fine sediment dynamics and morphology of major tropical deltas, such as the Mekong River, will respond to changing flow influences and coastal zones.

In this study, the Cape Ca Mau - Kien Giang (CM-KG) area of the Mekong Delta - located in the southwest of Vietnam with a coastline of more than 340 km, was selected. Here, many riverbank and coastal erosion occur every year and are on the rise [9]. The results of remote sensing image analysis in 2016-2020 show that the erosion trend has increased rapidly in the study area [22–25]. The CM-KG area has a shore retreat speed and ocean advance speed of -9.8 m/year and +24.3 m/year, with an average speed of 0.7 m/year. Erosions occurred strongly in 2018-2020, reflected in the area of land loss, increasing 2.7 times (from 250 hectares to 617 hectares) compared to 2016-2018. In 2016-2018, the area of accretion was up to 1122 hectares; however, by 2018-2020, the accretion area had decreased nearly ten times [26].

There have been many studies around the world using remote sensing image data to classify soil water from multi-temporal satellite images and then overlay them to identify and evaluate shoreline changes [27–29]. Specifically, the study [30] used Landsat 3, 5 and 8 images to create maps, calculate the rate of shoreline change in the Kanyakumari area - the southern boundary of India, located in Tamil Nadu and predict the period 2030-2040. The study [31] initial data was obtained from 1:25,000 topographic maps and multi-temporal satellite images (2006-2015) downloaded from the Google Earth archive focusing on the Kuwaru coastal area south of Yogyakarta special region facing the Indian Ocean. The study [4] the period (1990-2016) was analysed using Landsat 5, 7, and 8 images. The study focused on long-term coastal erosion analysis of the entire Karnataka coast. In Vietnam, research related to shoreline changes is of special interest. The study [32] Landsat seven images from 2001 to 2017 were used to evaluate Ca Mau coastal coastline changes using the Alesheikh ratio method (2006). The study [33] used the ENVI 4.7 tool to process remote sensing images and evaluate changes in the East and West coasts of Ca Mau. The study [34] researched using Landsat 8 images to assess changes in the Cua Dai coastline in 2016-2021 with a shoreline extraction technique based on two indices: AWEI index (*Automatic Water Extract Index*) and NDWI (*Normalization Differentiation Water Index*) and shoreline change calculation technique DSAS (*Digital Shoreline Analysis System*) [35].

In the above context, based on updated satellite data and remote sensing methods, this study clarified the sedimentation and erosion trends in the Western region - taking the coastal area of Ca Mau province - Kien Giang as a research case study. This study aims to clarify the range of accretion/erosion levels in the selected area, 2021-2023, using the integrated DSAS method, remote sensing, and GIS. The novelty of this research topic is reflected in the choice of research area and updated data. Previously, the west coast from Cape Ca Mau to Kien Giang was rarely chosen for a separate study. Meanwhile, the shoreline fluctuations in Dat Mui, Vien An (Ngoc Hien district), and Dat Moi (Nam Can district) communes are complicated by continuous sedimentation and erosion. The results show that applying remote sensing and GIS to assess shoreline changes is feasible and effective.

2. Materials and Methods

2.1. Study area

The research area is from Ngoc Hien district - Ca Mau, stretching to Ha Tien - Kien Giang. This area belongs to the Mekong Delta, mainly delta, with large estuaries and interlaced canals divided into ten sections corresponding to five Kien Giang and five districts of Ca Mau (Figure 1). Districts in Kien Giang province include Ha Tien-Kien

Luong, Hon Dat, Rach Gia, An Bien, and An Minh. Districts in Ca Mau province include U Minh, Phu Tan, Tran Van Thoi, Nam Can and Ngoc Hien.

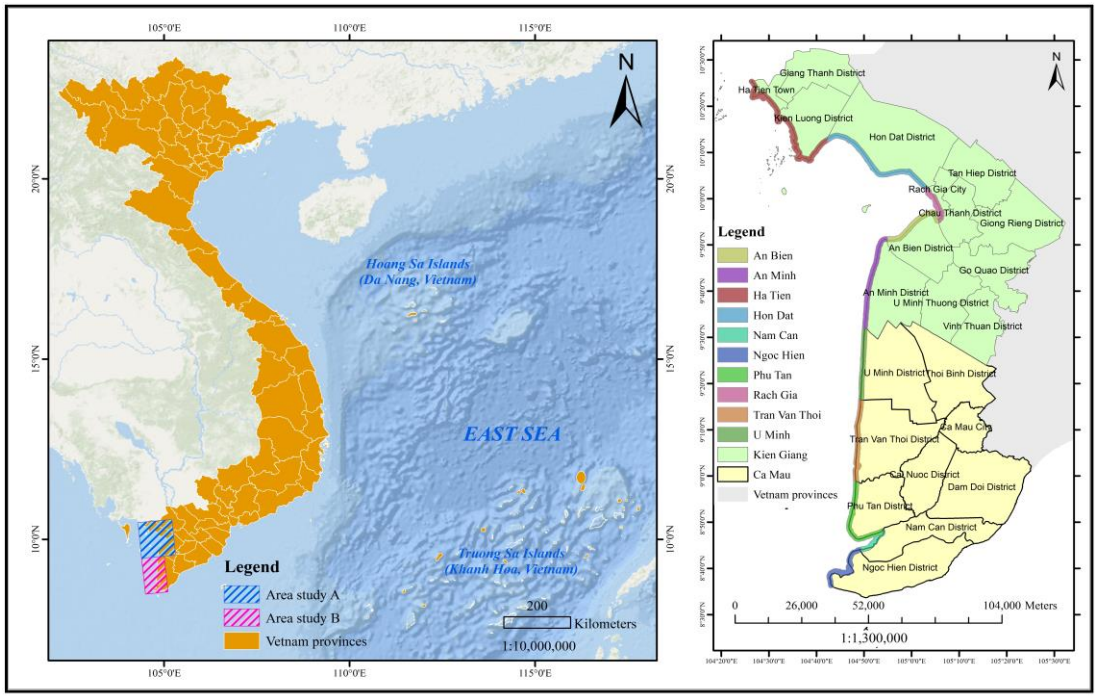

Figure 1. Study location map Ca Mau Cape - Kien Giang.

2.2. Data

The remote sensing images used in this study are Landsat8 OLI/TIRS Collection 2 Level 1 images from the Landsat 8 satellite launched on April 10, 2013. The United States Geological Survey - U.S. Geological Survey (USGS) provided the image free of charge from the website https://earthexplorer.usgs.gov/. Landsat8 OLI/TIRS Collection 2 Level 1 satellite images were taken in 11 image channels with different wavelengths and resolutions. However, the study only uses five image channels with a resolution of 30m × 30m, processed according to the WGS-84 UTM reference system, applied to area 49. Image interpretation results help evaluate erosion developments over time according to erosion area and distance parameters (Table 1). The satellite's imaging cycle is 16 days; a reasonable time to choose images is during the dry season months, with little rain and little cloud cover (Table 2).

Table 1. OLI and TIRs sensor characteristics of Landsat 8 satellite images [36].

Bands	**Wavelength** (micrometers)	**Resolution** (meters)
Band 1 - Coastal aerosol	0.43-0.45	30
Band 2 - Blue	0.45-0.51	30
Band 4 - Red	0.64-0.67	30
Band 5 - Near Infrared (NIR)	0.85-0.88	30
Band 7 - Shortwave Infrared (SWIR) 2	2.11-2.29	30

Table 2. Image data used in the study.

Year	**Day/month**	**Data set name**
2021	04/03	LC08_L1TP_126053_20210304_20210312_02_T1
	21/04	LC08_L1TP_126054_20210421_20210430_02_T1
2022	02/01	LC08_L1TP_126053_20220102_20220106_02_T1
	18/01	LC08_L1TP_126054_20220118_20220123_02_T1
2023	06/02	LC08_L1TP_126053_20230206_20230209_02_T1
	10/03	LC08_L1TP_126054_20230310_20230320_02_T1

2.3. Methods and implementation steps

In recent decades, remote sensing technology has developed rapidly as a tool to collect geospatial and atmospheric data with applications ranging from geoscience to economics. Currently, several methods are used to analyze coastline change, of which the Digital Shoreline Analysis System (DSAS) is considered an effective and widely used tool [31]. DSAS can integrate with ArcGIS software to analyze geographic information and calculate shoreline change rates in space and time. DSAS supports ArcGIS software to calculate the shoreline change rate over time by creating transect lines orthogonal to the set distance, thereby calculating the resulting shoreline change rate and matching the statistics in the attribute table. The distance between the transects is set, and the transects are constructed perpendicular to the Baseline baseline. The combination of DSAS and satellite images has been applied to several studies by [32–34]. Classifying surface cover types and analyzing changes is one of the most common applications of remote sensing. One of the most basic classification tasks is distinguishing water bodies from dry land surfaces. Landsat images are one of the most widely used data sources in remote sensing of water resources. The Automated Water Extraction Index (AWEI) was introduced to improve classification accuracy in areas with dark surfaces that other classification methods often fail to classify accurately [37]. The NDWI index (Normalized Difference Water Index - normalized difference water index) is often used to detect and distinguish areas with surface water from other objects [38]. In this study, the main steps include:

Step 1: After downloading and decompressing remote sensing images, they are inserted into ENVI 5.2 software to standardize the images. Convert the numerical values on the image to the value of physical radiation at the sensor. Then, the values of physical radiation at the sensor are converted to the value of reflection in the upper atmosphere of the object (object). AWEI calculation is essential to highlight land and water objects. Then, export the file in .tiff format and import it into ArcGIS to digitize the shoreline of the study area at the same scale. The result is to extract the shoreline for each year of study [25, 26].

Step 2: Use the DSAS tool to analyze accretion/erosion rates under the changes of the extracted shorelines. Calculate the distance and area of accretion/erosion over each year. Calculating and analyzing the shoreline is carried out as follows: Determine the baseline and calculated shorelines; Create transect lines perpendicular to the shore; Calculate the rate of shoreline change. Based on the collected data, the start-end rate (EPR) method was chosen to analyze the results. Formulas used: [25, 26]

EPR = Rate of change/ Total time to monitor changes (m/year)

where the rate of change is the distance between two coastlines, the total time of monitoring changes is the time between the oldest and newest coastlines [21].

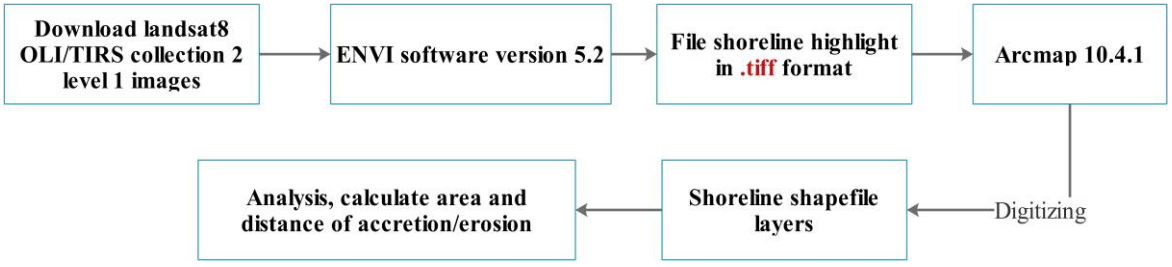

Figure 2. Study structure diagram.

3. Results and discussion

The area selected is a new land deposited by alluvium, formed by two ocean currents in the East Sea and the Gulf of Thailand, receiving alluvium from the Mekong River. The area is plain, has many rivers and canals, is a low, flat terrain, and is often flooded. The average height is 0.5m to 1.5m above sea level. The terrain direction gradually tilts from North to

South, from Northeast to Southwest. U Minh and Tran Van Thoi low-lying areas are inland "hanging depressions" limited by natural dikes of the Ong Doc, Cai Tau, and Trem river systems and high land edges along the West Coast. This hanging depression stagnates water all year round and becomes a swamp. The study of shoreline delineation and segmentation is shown in Figure 3; the results are analyzed and discussed in subsections.

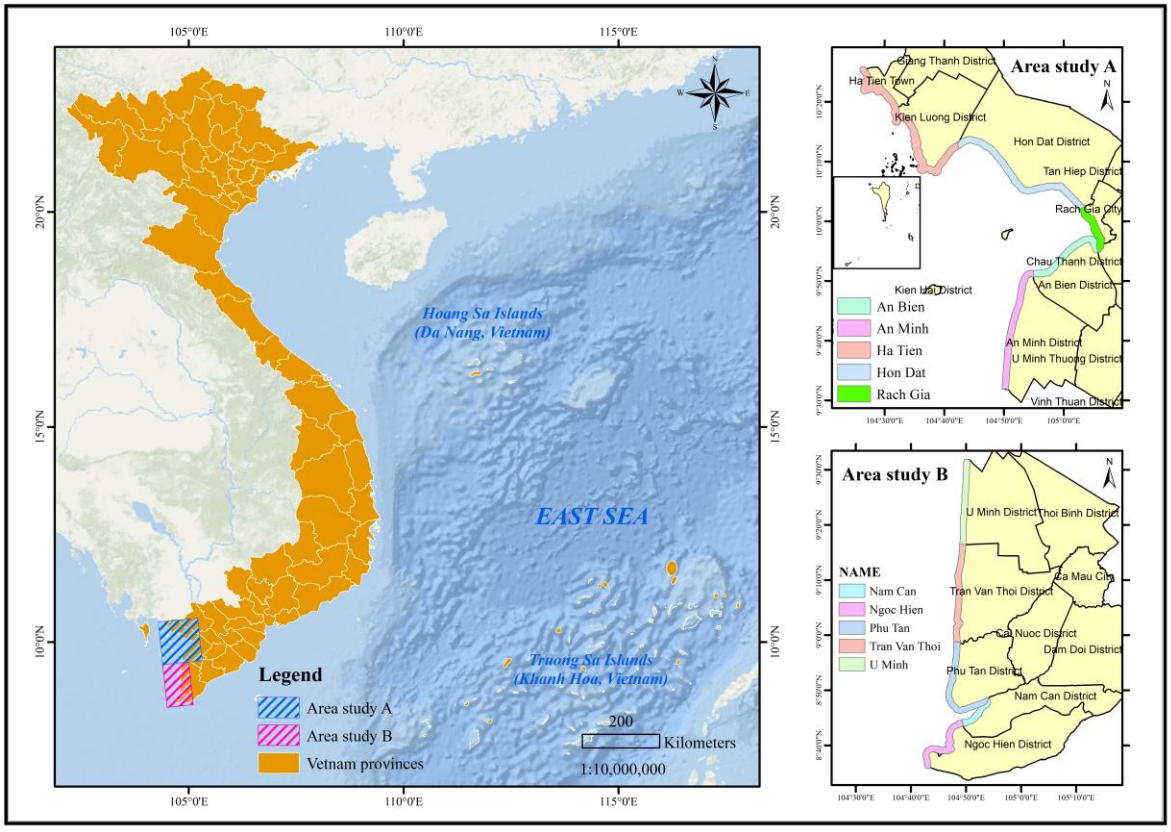

Figure 3. Delineation of the shoreline of typical accretion/erosion areas in Ca Mau - Kien Giang provinces in the period 2021-2023.

3.1. The accretion/erosion at Ha Tien - Kien Luong - Hon Dat districts

In Ha Tien - Kien Luong, in the period 2021-2022, the accretion/erosion rate is 18.08 m/year and 42.08 m/year, respectively, and the accretion/erosion area is 12.79 ha and 36.01 ha, respectively. In 2022-2023, the accretion/erosion rate is 11.34 m/year and 32.30 m/year, and the accretion/erosion area is 18.71 ha and 30.16 ha, respectively. In 2021-2023, the accretion/erosion rate is 11.16 m/year and 41.14 m/year, and the accretion/erosion area is 22.79 ha and 32.71 ha, respectively. Based on Figure 4A, the area of Binh An - Kien Luong commune is an erosion area.

At Hon Dat, in 2021-2022, the accretion/erosion rate is 19.49 m/year and 28.06 m/year, respectively, and the accretion/erosion area is 30.68 ha and 5.58 ha, respectively. In 2022-2023, the accretion/erosion rate is 18.56 m/year and 15.55 m/year, and the accretion/erosion area is 2.20 ha and 3.51 ha, respectively. In 2021-2023, the accretion/erosion rate is 17.60 m/year and 27.80 m/year, and the accretion/erosion area is 30.46 ha and 6.64 ha, respectively. Figure 4B clearly shows the erosion area in the Binh Giang and Binh Son commune. The results also show that between 2021-2022 and 2022-2023, the erosion rate will decrease, most clearly occurring in the area of Binh Giang commune and Binh Son commune; erosions only appear in Binh An commune. Some accretion locations are 2021-2022, accretion in Son Kien commune, and 2022-2023 in Binh Son commune (Figure 4C). The variation in accretion/erosion area is shown in Figure 4D.

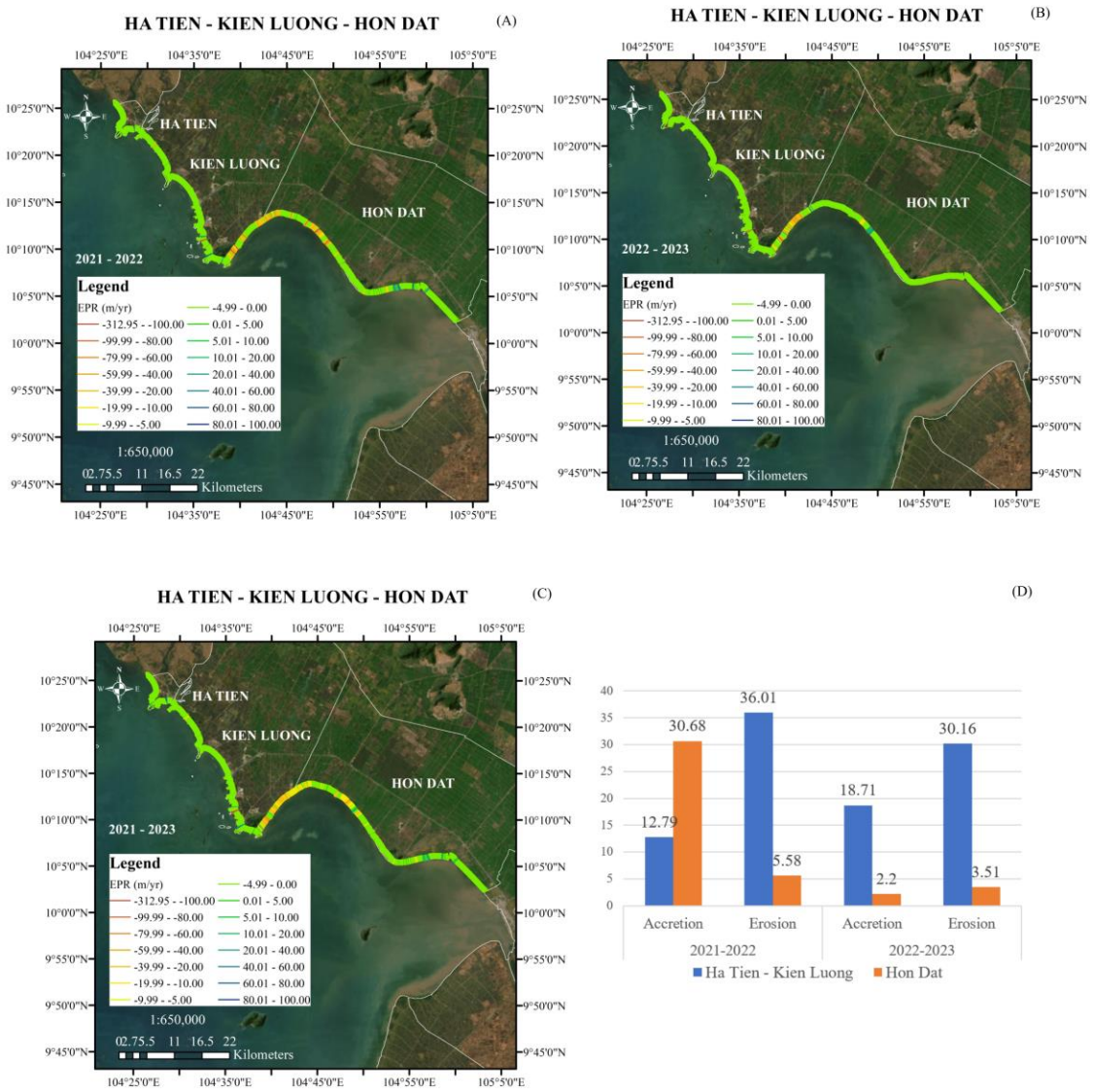

Figure 4. Map and chart showing erosion/accretion rate in TX. Ha Tien, Kien Luong, Hon Dat districts.

3.2. The accretion/erosion at Rach Gia - An Bien districts

In Rach Gia, in 2021-2022, the accretion/erosion rate is 11.16 m/year and 23.58 m/year, and the accretion/erosion area is 12.87 ha and 15.93 ha, respectively. In 2022-2023, the accretion/erosion rate is 16.43 m/year and 21.26 m/year, and the accretion/erosion area is 15.02 ha and 7.09 ha, respectively. In 2021-2023, the accretion/erosion rate is 15.40 m/year and 29.04 m/year, and the accretion/erosion area is 21.68 ha and 17.93 ha, respectively.

In An Bien, in 2021-2022, the accretion/erosion rate is 0.49 m/year and 42.94 m/year; the accretion/erosion area is 5.05 ha and 27.92 ha, respectively, Figure 5A. In 2022-2023, the accretion/erosion rate is 10.24 m/year and 24.96 m/year, and the accretion/erosion area is 9.39 ha and 17.24 ha, respectively. In 2021-2023, the accretion/erosion rate is 6.74 m/year and 26.27 m/year, and the accretion/erosion area is 9.21 ha and 29.59 ha, respectively. Based on Figure 5B, the Tay Yen commune area is an erosion area. The results show that the erosion rate will decrease between 2021-2022 and 2022-2023, most clearly in the Tay Yen - An Bien commune area. Some locations have accretion changes, such as erosions in 2021-2022 in An Hoa ward and accretion in 2022-2023. In Rach Soi ward, erosion has continuously increased over the years (Figure 5C). The variation in accretion/erosion area is shown in Figure 5D.

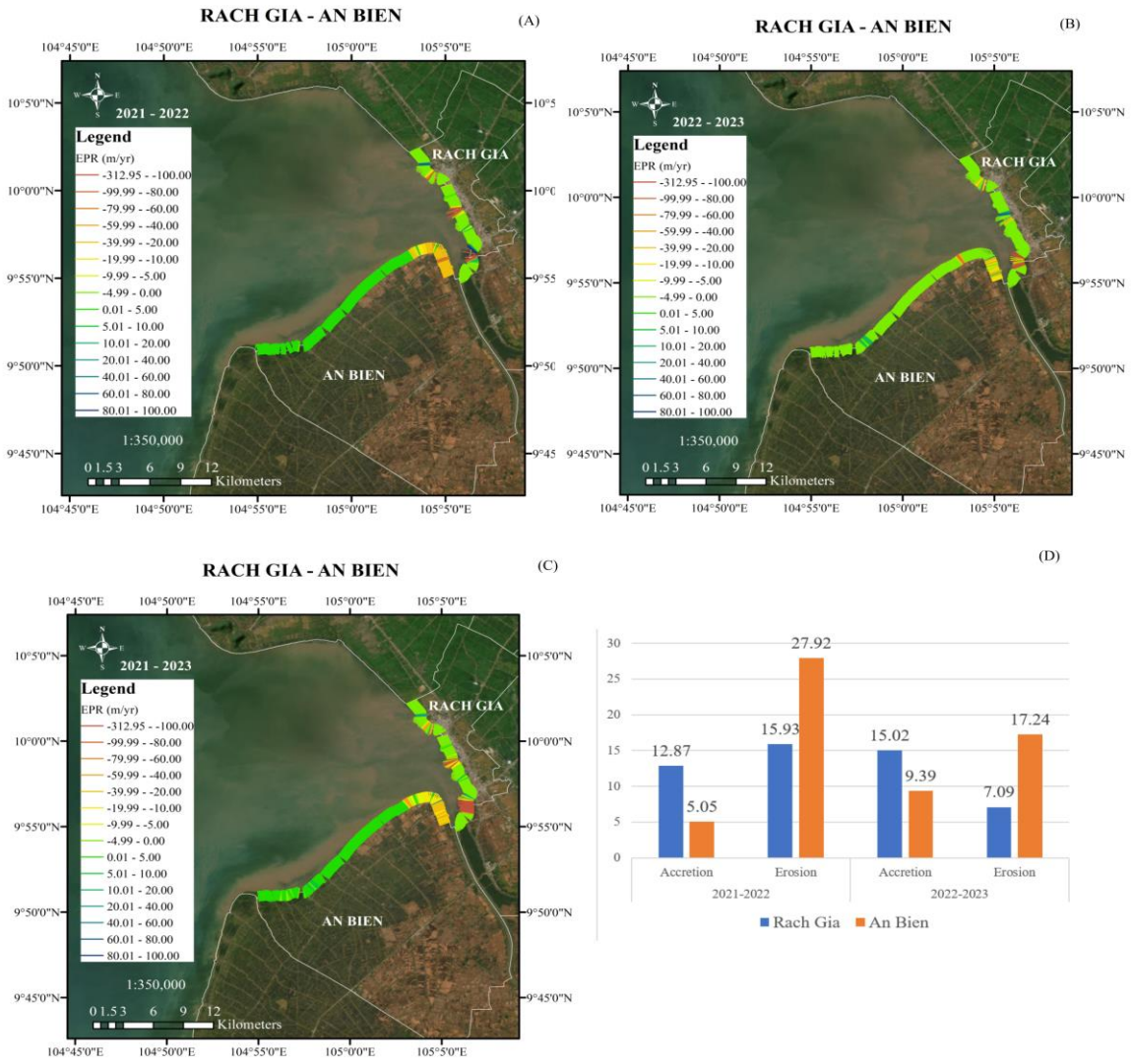

Figure 5. Map and chart showing erosion/accretion rate in Rach Gia, An Bien districts.

3.3. The accretion/erosion at An Minh - U Minh districts

In An Minh, in 2021-2022, the accretion/erosion rate is 15.87 m/year and 11.93 m/year, and the accretion/erosion area is 16.21 ha and 7.18 ha, respectively (Figure 6A). In 2022-2023, the accretion/erosion rate is 4.13 m/year and 18.94 m/year, and the accretion/erosion area is 0.79 ha and 2.32 ha, respectively (Figure 6B). In 2021-2023, the accretion/erosion rate is 8.48 m/year and 10.43 m/year, and the accretion/erosion area is 11.87 ha and 5.05 ha, respectively. Figure 6 shows the Van Khanh commune and Van Khanh Dong commune as accretional areas.

In U Minh, in 2021-2022, the accretion/erosion rate is 13.35 m/year and 6.77 m/year, and the accretion/erosion area is 10.25 ha and 6.61 ha, respectively (Figure 6A). In 2022-2023, the accretion/erosion rate is 12.57 m/year and 4.80 m/year, and the accretion/erosion area is 10.30ha and 4.87ha, respectively (Figure 6B). In 2021-2023, the accretion/erosion rate is 11.52 m/year and 8.85 m/year, and the accretion/erosion area is 10.06 ha and 5.12 ha, respectively (Figure 6C). Based on Figure 6, the area of Khanh Hoi commune and Khanh Tien commune is an accretion area.

Analysis results show that erosion and accretion are interwoven in An Minh-U Minh, but accretion is predominant. Between 2021-2022 and 2022-2023, the accretion rate in this area decreased, but An Minh district only has an increased erosion rate. The variation in accretion/erosion area is shown in Figure 6D.

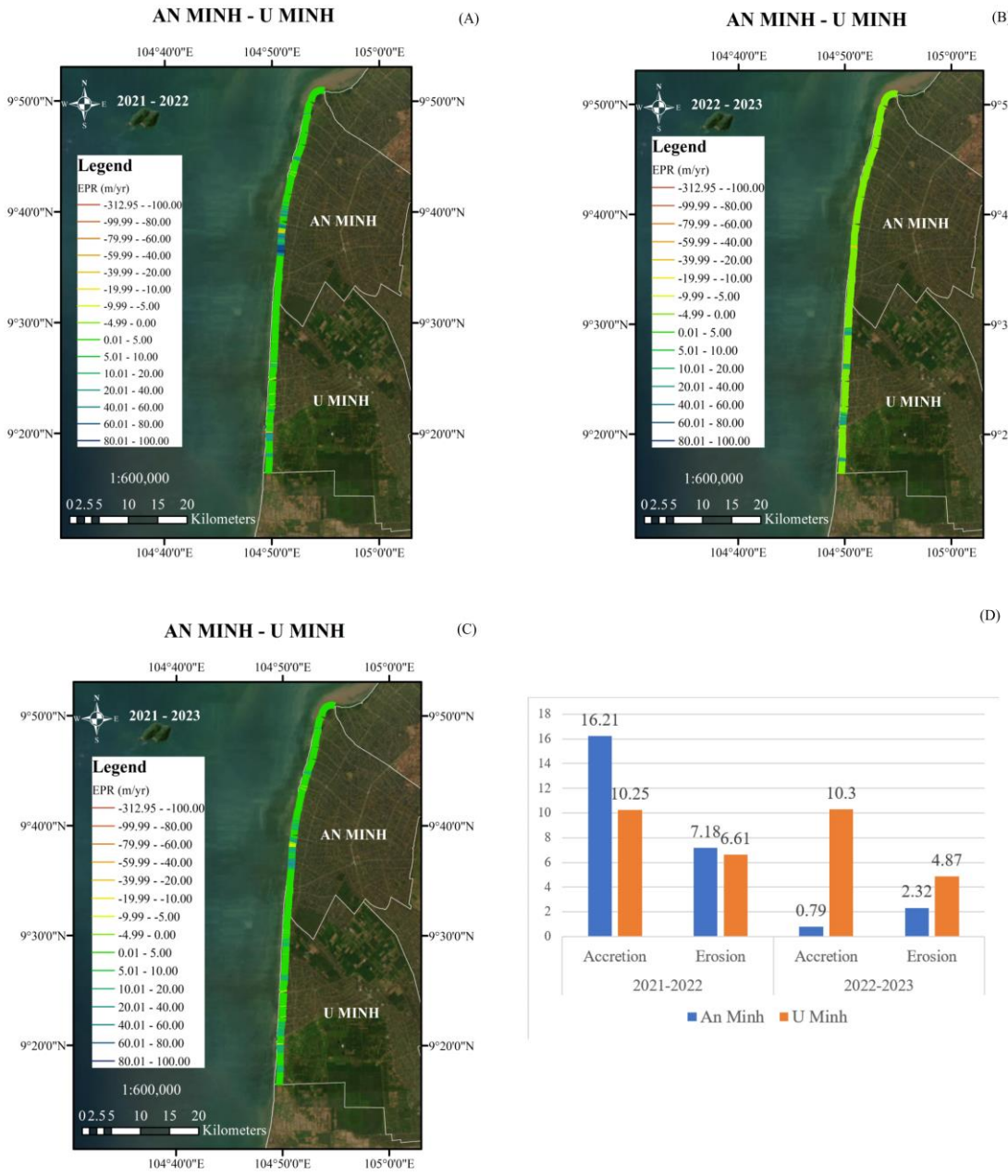

Figure 6. Map and chart showing erosion/accretion rate in An Minh and U Minh districts.

3.4. The accretion/erosion at Tran Van Thoi district

At Tran Van Thoi, in 2021-2022, the accretion/erosion rate is 19.41 m/year and 7.02 m/year, and the accretion/erosion area is 20.05 ha and 3.36 ha, respectively (Figure 7A). In 2022-2023, the accretion/erosion rate is 16.29 m/year and 5.55 m/year, and the accretion/erosion area is 26.17 ha and 4.95 ha, respectively (Figure 7B). In 2021-2023, the accretion/erosion rate will be 17.65 m/year and 6.49 m/year, and the accretion/erosion area will be 19.99 ha and 5.24 ha, respectively. Figures 7A-C show that the area of Khanh Hai commune, Song Doc town, and Phong Dien commune is the accretional area. The variation in accretion/erosion area is shown in Figure 7D.

Analysis results show that erosion and accretion are interwoven in the Tran Van Thoi area, but accretion is the main. Although the accretion rate will decrease between 2021-2022 and 2022-2023, the accretion area will still increase, and the erosion area will increase slightly. The variation in accretion/ erosion area is shown in Figure 7D.

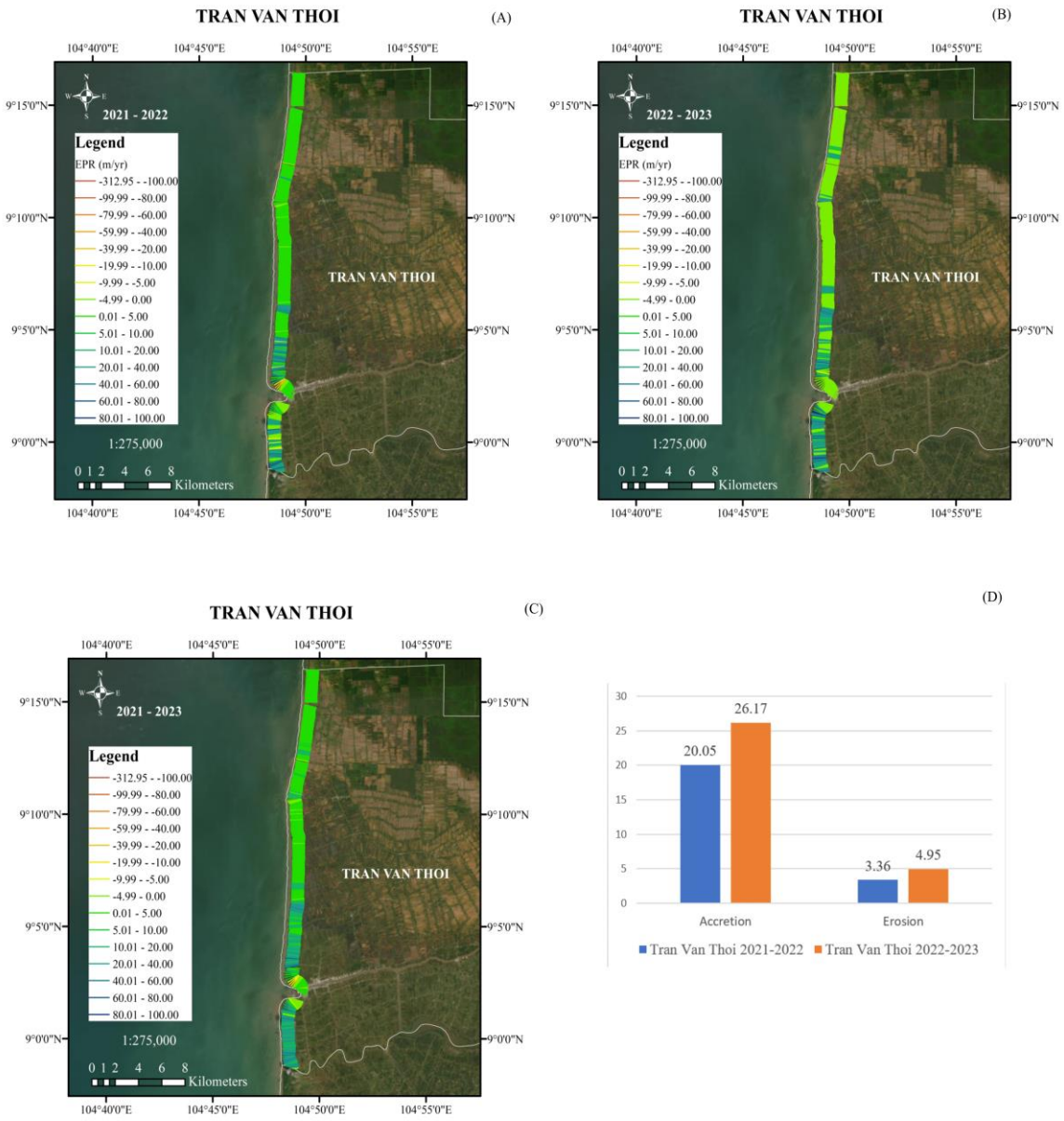

Figure 7. Map and chart showing erosion/accretion rate in Tran Van Thoi district.

3.5. The accretion/erosion at Phu Tan - Nam Can - Ngoc Hien districts

In Phu Tan, in 2021-2022, the accretion/erosion rate is 15.39 m/year and 10.04 m/year, and the accretion/erosion area is 30.71 ha and 8.03 ha, respectively. In 2022-2023, the accretion/erosion rate is 13.74 m/year and 4.39m/year, and the accretion/erosion area is 40.80 ha and 5.18 ha, respectively. In 2021-2023, the accretion/erosion rate is 15.95m/year and 9.30m/year, and the accretion/erosion area is 30.68 ha and 7.87 ha, respectively. Figure 6 shows the area of Phu Tan commune to Cai Doi Vam commune shows an accretion trend but is still slightly eroded.

In Nam Can, in 2021-2022, the accretion/erosion rate is 10.95 m/year and 37.73 m/year, and the accretion/erosion area is 3.67 ha and 10.52 ha, respectively Figure 8 A. In 2022-2023, the accretion/erosion rate is 8.92 m/year and 25.99 m/year, respectively, and the accretion/erosion area is 4.23 ha and 26.39 ha, Figure 8B. In 2021-2023, the accretion/erosion rate is 9.34 m/year and 33.88 m/year; the accretion/erosion area is 4.61 ha and 32.71 ha, respectively. The results shown in Figure 8 show that the areas of Dat Moi and Lam Hai communes have an erosion trend.

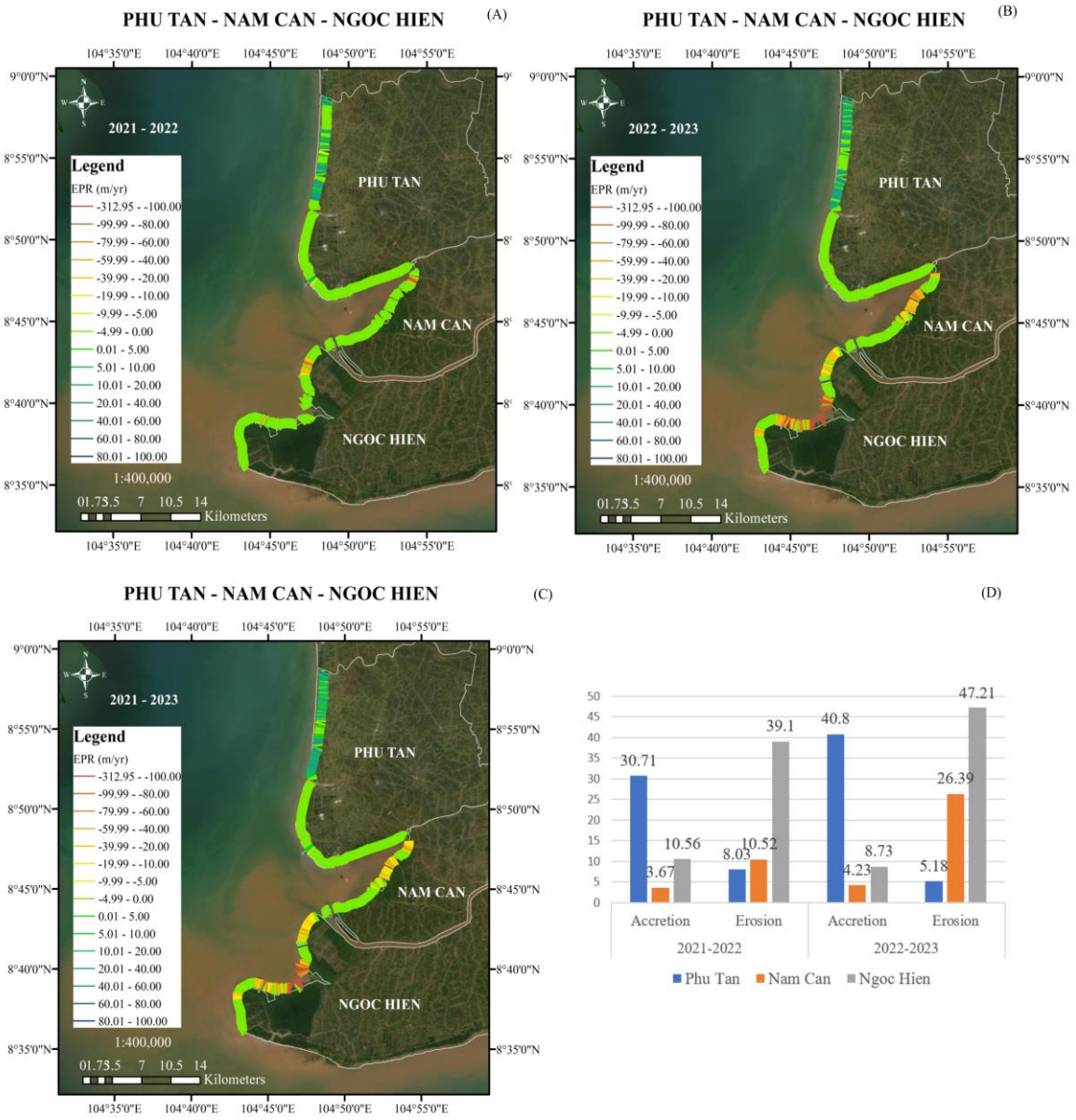

Figure 8. Map and chart showing erosion/accretion rates in Phu Tan, Nam Can and Ngoc Hien districts.

In Ngoc Hien, in 2021-2022, the accretion/erosion rate is 16.89 m/year and 36.53 m/year, respectively, and the accretion/erosion area is 10.56 ha and 39.10 ha, respectively. In 2022-2023, the accretion/erosion rate is 9.09 m/year and 55.66 m/year, and the accretion/erosion area is 8.73 ha and 47.21 ha, respectively. In 2021-2023, the accretion/erosion rate is 11.55 m/year and 47.79 m/year, and the accretion/erosion area is 9.39ha and 44.73 ha, respectively. The interpretation results in Figure 8 show that the areas of Vien An and Dat Mui communes are severely eroded.

General assessment shows that erosion and accretion are complexly interwoven yearly at Phu Tan - Nam Can - Ngoc Hien. In both periods, Phu Tan district was mainly accreted from Phu Tan commune to Cai Doi Vam commune. In 2021-2022, erosion will occur in Dat Moi - Nam Can commune and Vien An - Ngoc Hien commune area. By 2022-2023, erosion will expand further in Dat Moi commune, Lam Hai commune - Nam Can and is especially serious in Ngoc Hien district, from Vien An commune to Dat Mui commune. The variation in accretion/erosion area is shown in Figure 8D.

4. Conclusion

Evaluation results based on the shoreline extraction technique using the AWEI index and DSAS tool to calculate the current state of the shoreline over the years clearly show the trend of erosion/accretion on the coast of the Mekong Delta, the section from Ca Mau Cape to Kien Giang.

Although the trends of accretion/erosion in the study area are mixed, in the study period 2021-2023, the total area of accretion is 170.74 hectares, while the total area of erosion is 257.34 hectares. Thus, the increasing trend of erosion is a potential risk for the area. The results also show that the area of land loss in 2022-2023 is 115.43 hectares, an increase compared to the area of land loss in 2021-2022 of 109.37 hectares.

Next, it is necessary to clarify the mechanism of the formation of erosion and accretion zones by modelling seasonal hydrodynamic factors and mud and sediment factors received from the upstream to the river mouth. From the above results, we can determine the importance of applying remote sensing image analysis combined with GIS to monitor coastline changes. This method gives quick results and is less time-consuming but still ensures results, so this will be a helpful choice in shoreline protection, prevention, and management.

Author contribution statement: Developing research ideas, drawing up a draft writing plan, editing the manuscript, revising the manuscript version: L.T.B.; Process data: processing, first manuscript writing: D.C.M.N; GIS, Process data: V.H.T.D.

Acknowledgments: This research was funded by Vietnam National University Ho Chi Minh city (VNU-HCM), grant No: B2023-20-23. The authors would like to thank the Ho Chi Minh City University of Technology for the support of time and facilities from the Ho Chi Minh City University of Technology (HCMUT), VNU-HCM for this study.

Competing interest statement: The authors declare no conflict of interest.

References

1. Uścinowicz, G.; Uścinowicz, S.; Szarafin, T.; Maszloch, E.; Wirkus, K. Rapid coastal erosion, its dynamics and cause – An erosional hot spot on the southern Baltic Sea coast. *Oceanologia* **2023**. doi: 10.1016/j.oceano.2023.12.002.
2. Agate, J.; Ballinger, R.; Ward, R.D. Estuarine, coastal and shelf science satellite remote sensing can provide semi-automated monitoring to aid coastal decision-making. *Estuar. Coast. Shelf Sci.* **2024**, *298(8)*, 108639. doi: 10.1016/j.ecss.2024.108639.
3. Senevirathna, E.M.T.K.; Edirisooriya, K.V.D.; Uluwaduge, S.P.; Wijerathna, K.B.C.A. Analysis of causes and effects of coastal erosion and environmental degradation in southern coastal belt of Sri Lanka special reference to unawatuna coastal area. *Procedia Eng.* **2018**, *212*, 1010–1017. doi: 10.1016/j.proeng.2018.01.130.
4. Sowmya, K.; Sri, M.D.; Bhaskar, A.S.; Jayappa, K.S. Long-term coastal erosion assessment along the coast of Karnataka, west coast of India. *Int. J. Sediment Res.* **2019**, *34(4)*, 335–344. doi: 10.1016/j.ijsrc.2018.12.007.
5. Neelamani, S. Coastal erosion and accretion in Kuwait - Problems and management strategies. *Ocean Coast. Manag.* **2018**, *156*, 76–91. doi: 10.1016/j.ocecoaman.2017.05.014.
6. George, L.; Androws, X.; Krishnan, A.; Kumar, A.; Kannan, R.; Muthusankar, G.; Balasubramani, K. Assessment of shoreline changes and associated erosion and accretion pattern in coastal watersheds of Tamil Nadu, India. *Nat. Hazards Res.* **2023**. doi: 10.1016/j.nhres.2023.09.008.
7. Schmitt, K.; Albers, T. Area coastal protection and the use of bamboo breakwaters in the Mekong Delta. *Coastal Disasters Clim. Change VN Eng. Plann. Perspect.* **2014**, 107–132.
8. Nhan, N.H. Synthesis report of the formation and development mechanism of coastal accretion areas and scientific and technological solutions for sustainable socio-

economic development in Ca Mau coastal area-Code:ĐTĐL.2011.T/43. (In Vietnamse). Ho Chi Minh City, 2015.

9. Anthony, E.J.; Brunier, G.; Besset, M.; Goichot, M.; Dussouillez, P.; Lap, N.V. Linking rapid erosion of the Mekong River delta to human activities. *Sci. Rep.* **2015**, *5*, 4–9. doi: 10.1038/srep14745.
10. Brunier, G.; Anthony, E.J.; Goichot, M.; Provansal, M.; Dussouillez, P. Recent morphological changes in the Mekong and Bassac river channels, Mekong delta: The marked impact of river-bed mining and implications for delta destabilisation. *Geomorphology* **2014**, *224*, 177–191. doi: 10.1016/j.geomorph.2014.07.009.
11. Manh, N.V.; Dung, N.V.; Hung, N.N.; Kummu, M.; Merz, B.; Apel, H. Future sediment dynamics in the Mekong Delta floodplains: Impacts of hydropower development, climate change and sea level rise. *Glob. Planet. Change*. **2015**, *127*, 22–33. doi: 10.1016/j.gloplacha.2015.01.001.
12. Gugliotta, M.; Saito, Y.; Nguyen, V.L.; Ta, T.K.O.; Nakashima, R.; Tamura, T.; Uehara, K.; Katsuki, K.; Yamamoto, S. Process regime, salinity, morphological, and sedimentary trends along the fluvial to marine transition zone of the mixed-energy Mekong River delta, Vietnam. *Cont. Shelf Res*. **2017**, *147*, 7–26. doi: 10.1016/j.csr.2017.03.001.
13. McLachlan, R.L.; Ogston, A.S.; Allison, M.A. Implications of tidally-varying bed stress and intermittent estuarine stratification on fine-sediment dynamics through the Mekong's tidal river to estuarine reach. *Cont. Shelf Res.* **2017**, *147*, 27–37. doi: 10.1016/j.csr.2017.07.014.
14. Xing, F.; Meselhe, E.A.; Allison, M.A.; Weathers, H.D. Analysis and numerical modeling of the flow and sand dynamics in the lower Song Hau channel, Mekong Delta. *Cont. Shelf Res.* **2017**, *147*, 62–77. doi: 10.1016/j.csr.2017.08.003.
15. Vo, Q.T.; Reyns, J.; Wackerman, C.; Eidam, E.F.; Roelvink, D. Modelling suspended sediment dynamics on the subaqueous delta of the Mekong River. *Cont. Shelf Res.* **2017**, *147(7)*, 213–230. doi: 10.1016/j.csr.2017.07.013.
16. Ogston, A.S.; Allison, M.A.; Mullarney, J. C.; Nittrouer, C.A. Sediment and hydro-dynamics of the Mekong Delta: From tidal river to continental shelf. *Cont. Shelf Res.* **2017**, *147*, 1–6. doi: 10.1016/j.csr.2017.08.022.
17. Thai, N.H.; Thuy, N.B.; Dang, V.H.; Kim, S.; Hole, L.R. Impact of the interaction of surge, wave and tide on a storm surge on the north coast of Vietnam. *Procedia IUTAM* **2017**, *25*, 82–91. doi: 10.1016/j.piutam.2017.09.013.
18. Loisel, H.; Mangin, A.; Vantrepotte, V.; Dessailly, D.; Dinh, D.N.; Garnesson, P.; Ouillon, S.; Lefebvre, J.P.; Mériaux, X.; Phan, T.M. Variability of suspended particulate matter concentration in coastal waters under the Mekong's influence from ocean color (MERIS) remote sensing over the last decade. *Remote Sens. Environ.* **2014**, *150*, 218–230. doi: 10.1016/j.rse.2014.05.006.
19. Liu, C.; He, Y.; Des, E.W.; Wang, J. Changes in the sediment load of the Lancang-Mekong River over the period 1965-2003. *Sci. China Technol. Sci.* **2013**, *56(4)*, 843–852. doi: 10.1007/s11431-013-5162-0.
20. Heege, T.; Kiselev, V.; Wettle, M.; Hung, N.N. Operational multi-sensor monitoring of turbidity for the entire Mekong Delta. *Int. J. Remote Sens.* **2014**, *35(8)*, 2910–2926. doi: 10.1080/01431161.2014.890300.
21. Fleifle, A.E. Suspended Sediment Load Monitoring Along the Mekong River from Satellite Images. *J. Earth Sci. Clim. Change* **2013**, *04(06)*, 160. doi: 10.4172/2157-7617.1000160.
22. Hoang, T.B. Research and find solutions and technologies to prevent river bank erosion in Bac Lieu and Ca Mau provinces. Report Scientific Conference 12/27/2017: Southern institute of water resources research, HCM city, 2017.
23. Linh, B.; Bui, L. Modelling bank erosion dependence on natural and anthropogenic factors – Case study of Ganh Hao estuary, Bac Lieu - Ca Mau, Vietnam. *Environ. Technol. Innov.* **2020**, *19*, 100975. doi: 10.1016/j.eti.2020.100975.

24. Xuan, N.T.; Duyen, C.M.N.; Long, B.T. Simulating $PM_{2.5}$ dust pollution and analyzing related factors – The case of Ca Mau province, Vietnam. *J. Hydro-Meteorol.* **2023**, *756(12)*, 42–58.
25. Phuong, P.V.T.; Hanh, P.T.H.; Long, B.T. Application of remote sensing, GIS to assess the rate and range of coastal erosion in the Mekong River Delta, from Tien Giang to Soc Trang Province. *VN J. Hydrometeorol.* **2023**, *754*, 9–25. doi: 10.36335/vnjhm.2023.(754).9-25.
26. Pham, H.T.H.; Bui, L.T. Mechanism of erosion zone formation based on hydrodynamic factor analysis in the Mekong Delta coast, Vietnam. *Environ. Technol. Innov.* **2023**, *30*, 103094. doi: 10.1016/j.eti.2023.103094.
27. Hoang, T.T.; Dao, K.N.; Pham, L.T.; Van, N.H. Analysis of riverbank changes in Ho Chi Minh city in the period 1989 - 2015. *Sci. Technol. Dev. J. Sci. Earth Environ.* **2019**, *2(2)*, 80–88. doi: 10.32508/stdjsee.v2i2.496.
28. Elkafrawy, S.B.; Basheer, M.A.; Mohamed, H.M.; Naguib, D.M. Applications of remote sensing and GIS techniques to evaluate the effectiveness of coastal structures along Burullus headland-Eastern Nile Delta, Egypt. *Egypt. J. Remote Sens. Sp. Sci.* **2021**, 24(2), 247–254. doi: 10.1016/j.ejrs.2020.01.002.
29. Attar, I.M.S.A.; Basheer, M.A. Multi-temporal shoreline analysis and future regional perspective for Kuwait coast using remote sensing and GIS techniques. *Heliyon*. **2023**, *9(9)*, e20001. doi: 10.1016/j.heliyon.2023.e20001.
30. Chrisben, S.S.; Gurugnanam, B. Coastal transgression and regression from 1980 to 2020 and shoreline forecasting for 2030 and 2040, using DSAS along the southern coastal tip of Peninsular India. *Geod. Geodyn.* **2022**, *13(6)*, 585–594. doi: 10.1016/j.geog.2022.04.004.
31. Mutaqin, B.W. Shoreline changes analysis in Kuwaru coastal area, Yogyakarta, Indonesia: An application of the digital shoreline analysis system (DSAS). *Int. J. Sustain. Dev. Plan.* **2017**, *12(7)*, 1203–1214. doi: 10.2495/SDP-V12-N7-1203-1214.
32. Tinh,T.V.; Phong, D.H. Applying remote sensing and gis for study change in coastal areas of Ca Mau cap. *VN J. Hydrometeorol*. **2017**, *684*, 41–53.
33. Thanh, N.T. Analysis and evaluation of erosion and deposition processes in Ca Mau by remote sensing and GIS. *VN J. Hydrometeorol*. **2021**, *721*, 66–79. doi: 10.36335/vnjhm.2021(721).66-79.
34. Quynh, C.K.N.; Hanh, P.T.H.; Long, B.T. Assessment of the shoreline evolution and coastal erosion trends along Cua Dai beach, Hoi An City, Quang Nam. *VN J. Hydrometeorol.* **2022**, *736(1)*, 41–53. doi: 10.36335/VNJHM.2022(736(1)).41-53.
35. Thin, V.T.; Duan, P.V.; Thi, N.V.; Hung, N.V.; Van, N.H. Landsat8 disposal service photo identification phase fluctuations and coating plant. *J. Forestry. Sci. Technol*. **2015**, *N1*, 73–83.
36. U.D. of the Interior. What are the band designations for the Landsat satellites? USGS, 2014.
37. Feyisa, G.L.; Meilby, H.; Fensholt, R.; Proud, S.R. Automated Water Extraction Index: A New Technique for Surface Water Mapping Using Landsat Imagery. *Remote Sens. Environ.* **2014**, 23–35. doi: 10.1016/j.rse.2013.08.029.
38. Teng, J.; Xia, S.; Liu, Y.; Yu, X.; Duan, H.; Xiao, H.; Zhao, C. Assessing habitat suitability for wintering geese by using normalized difference water index (NDWI) in a large floodplain wetland, China. *Ecol. Indic.* **2021**, *122*, 107260. doi: 10.1016/j.ecolind.2020.107260.